

# Golden Binary Gravitational-wave Sources: Robust Probes of Strong-Field Gravity

Scott A. Hughes<sup>1</sup> & Kristen Menou<sup>2</sup>

## ABSTRACT

Space-born gravitational-wave interferometers such as *LISA* will detect the gravitational wave (GW) signal from the inspiral, plunge and ringdown phases of massive black hole binary mergers at cosmological distances. From the inspiral waves, we will be able to measure the masses of the binaries' members; from the ringdown waves, we will be able to measure the mass of the final merged remnant. A subset of detected events allow the identification of both the inspiral and the ringdown waveforms in a given source, and thus allow a measurement of the total mass-energy lost to GWs over the coalescence,  $M_{\text{GW}}$ . We define “golden” binary mergers to be those with measurement errors likely to be small enough for a physically useful determination of  $M_{\text{GW}}$ . A detailed sensitivity study, combined with simple black hole population models, suggests that a few golden binary mergers may be detected during a 3-year *LISA* mission lifetime. Any such mass deficit measurement would constitute a robust and valuable observational test of strong-field relativistic gravity. An extension of this concept to include spin measurements may allow a direct empirical test of the black hole area theorem.

*Subject headings:* black hole physics – cosmology: theory – quasars: general – galaxies: active, nuclei, interactions – gravitation – relativity

## 1. Introduction

The Laser Interferometer Space Antenna (*LISA*), a joint ESA and NASA enterprise, is due for launch around the year 2013. One of its main science objectives is the direct detection of gravitational waves (GWs) from coalescing massive black holes (MBHs) at cosmological

---

<sup>1</sup>Department of Physics and Center for Space Research, Massachusetts Institute of Technology, 77 Massachusetts Avenue, Cambridge, MA 02139, USA

<sup>2</sup>Department of Astronomy, Columbia University, 550 West 120th Street, New York, NY 10027, USA

distances<sup>1</sup>. Although the mission concept has not yet been entirely finalized, it is already possible to estimate the accuracy with which *LISA* will measure a variety of observables related to MBH coalescences. For example, several groups have made predictions for the rate of MBH mergers detectable by *LISA* under various assumptions for the underlying cosmological model of BH mass assembly (see, e.g., Haehnelt 1994; Menou, Haiman & Narayanan 2001; Wyithe & Loeb 2003; Islam, Taylor & Silk 2004; Sesana et al. 2004a,b).

These measurements will provide rich information about the binary generating the GW signal. Hughes (2002) has presented detailed calculations of the exquisite precision with which *LISA* will measure MBH masses in equal-mass mergers, as a function of redshift. Vecchio (2004) has shown that Hughes’ estimates are in fact fairly pessimistic: by taking into account spin-induced precessional effects in the binary coalescence, mass measurements can be improved. It should even be possible to extract useful information about the spins of the binary’s members.

In this analysis, we focus on a specific class of MBH binaries that we label “golden” binaries. These are binaries for which *LISA* will witness the entire coalescence, from inspiral to plunge and ensuing ringdown. In these events, the masses of the binary’s BH components before merger and of the final merged remnant can each be measured to high precision. Because GWs carry mass-energy from the system, the system’s final mass  $M_f$  will be less than the initial mass  $M_i$  it has when the binary’s members are widely separated. For golden binaries, the masses are determined so precisely that the total mass deficit due to GW emission,  $M_{\text{GW}} \equiv M_i - M_f$ , can potentially be determined observationally.

Such a measurement would constitute a very robust test of a strikingly strong-field prediction of general relativity. At present, theory does not tell us too much about  $M_{\text{GW}}$  in general, though we have information about some idealized cases, such as extreme mass ratios (e.g., Davis et al 1971, Nakamura, Oohara, & Kojima 1987). Much effort is being directed towards improving this situation, both via large scale numerical efforts (see Baumgarte & Shapiro 2003 for a review, or Brüggmann, Tichy, & Jansen 2004 for a snapshot of recent progress) and analytical calculations (Damour 2001). It is thus obviously of great interest to understand what direct observational constraints can be obtained about this process as it occurs in nature.

We show that for the golden binaries *LISA* has the capability to measure mass deficits in cosmic MBH mergers to high enough accuracy that strong-field general relativity can be tested. A particularly noteworthy feature of this measurement is that our calculation relies only on parameters measured during the “inspiral” (when the binary’s members are

---

<sup>1</sup>See <http://lisa.nasa.gov/>

widely separated and slowly spiraling towards one another due to the backreaction of GW emission) and during the “ringdown” (the last dynamics of the system, generated after the binary’s holes have merged and are settling down to a quiescent Kerr black hole state). No information about the highly dynamical final plunge and “merger” process is needed. In this sense, measurement of  $M_{\text{GW}}$  from golden binaries is very robust, and will thus constitute a particularly simple but powerful probe of strong-field gravity. We argue that it is not unreasonable to expect *LISA* to perform such measurements for a 3-year mission life-span.

In §2, we describe the parameterized gravitational waveform upon which we base our analysis. We describe in some detail the forms we use for the inspiral and ringdown waves, outlining how they depend upon and thus encode the binary’s masses. It’s worth noting that the functional form of the inspiral waves that we use does not take into account precessional effects that arise due to spin-orbit and spin-spin interactions. A substantial improvement in mass determination during the inspiral can be obtained by taking this effect into account; the spins of the binary’s members can thereby be measured as well. This comes, however, with a substantial increase in waveform complexity and thus computational cost (Vecchio 2004). It is worth emphasizing this point since it is likely that our estimates of how accurately  $M_{\text{GW}}$  is measured are somewhat pessimistic due to our reliance on this relatively crude parameterization.

In §3, we describe the calculation we perform to estimate how accurately  $M_{\text{GW}}$  can be measured. What is clear from the modeling that has been done to date is that  $M_{\text{GW}}$  is a fairly small fraction of the binary’s total mass — at most, 10 – 20% of the total binary mass  $M$  is radiated away over the entire coalescence. In order for a determination of  $M_{\text{GW}}$  to be meaningful, the error  $\delta M_{\text{GW}}$  must be substantially smaller than  $M_{\text{GW}}$  itself. We (somewhat arbitrarily) define the regime of golden binaries to be those for which  $\delta M_{\text{GW}}/M \simeq 5\%$  or less. We construct the error  $\delta M_{\text{GW}}$  from errors in the mass parameters measured by the inspiral [the “chirp mass” and reduced mass, defined in Eq. (2)] and the ringdown (the final mass of the system). We outline how this error is calculated using a standard maximum-likelihood measurement formalism (Finn 1992). We then perform a large number of Monte-Carlo simulations to assess how well  $M_{\text{GW}}$  can be measured as a function of source masses and redshift. We find that binaries with total mass  $M$  in the (very rough) range several  $\times 10^5 M_{\odot} \lesssim M \lesssim$  a few  $\times 10^6 M_{\odot}$  have the potential to be golden out to a redshift  $z \sim 3 - 4$ .

In §4, we calculate event rates for golden binary mergers. The specific population models we use are based on a merger tree describing dark matter halo evolution in a concordance  $\Lambda$ -CDM cosmology. This scenario suggests that *LISA* should plausibly be able to measure several golden events during its mission lifetime. We conclude in §5 with a discussion of the

limitations of and possible extensions to our work.

## 2. Model for the coalescence waves

As is common, we break the binary black hole coalescence process into three more-or-less distinct epochs — the *inspiral*, *merger*, and *ringdown*. We briefly describe these three epochs, sketching the gravitational waveforms each produces and how they encode source parameters. It should be emphasized that this characterization is rather crude. The delineation between “inspiral” and “merger” in particular is not very clear cut, especially when a binary’s members are of comparable mass. Despite its crudeness, it is a very useful characterization for our purposes, since parameterized waveforms exist for the inspiral and ringdown epochs.

### 2.1. Inspiral

“Inspiral” denotes the epoch in which the black holes are widely separated from one another and slowly spiral together due to the backreaction of gravitational waves upon the system. These GWs are well modeled (at least over most of this epoch) using the post-Newtonian approximation to general relativity, roughly speaking an expansion in inverse separation of the bodies; see Blanchet (2002) and references therein for more detailed discussion.

The strongest harmonic of the inspiral waves has the form

$$h_{\text{insp}}(t) = \frac{\mathcal{M}_z^{2/3} f(t)^{2/3}}{D_L} \mathcal{F}(\text{angles}) \cos [\Phi(t)] , \quad (1)$$

where  $\mathcal{M}_z$  is the redshifted “chirp mass” (described in the following paragraph),  $D_L$  is the luminosity distance to the source,  $\Phi(t)$  is the accumulated GW phase, and  $f(t) = (1/2\pi)d\Phi/dt$  is the GW frequency. The function  $\mathcal{F}(\text{angles})$  stands for the rather complicated dependence of the signal on the position and orientation angles of the source; see Cutler (1998) for a detailed discussion of this dependence.

The phase function  $\Phi$  depends very strongly upon the source’s chirp mass  $\mathcal{M}$  (so called because it largely determines the rate at which a binary’s orbital frequency changes), and somewhat less strongly upon the reduced mass  $\mu$ . These mass parameters relate to the masses which a binary’s black holes would have in isolation,  $m_1$  and  $m_2$ , by

$$\mathcal{M} = \frac{(m_1 m_2)^{3/5}}{(m_1 + m_2)^{1/5}} , \quad \mu = \frac{m_1 m_2}{m_1 + m_2} . \quad (2)$$

A measurement of  $\mathcal{M}$  and  $\mu$  can thus determine the isolated black hole masses,  $m_1$  and  $m_2$ , fixing the initial mass  $M_i = m_1 + m_2$ . The phase  $\Phi$  is the observable to which GW measurements are most sensitive. By measuring this phase and fitting to a model (“template”), one can infer the source’s physical parameters. Since  $\mathcal{M}$  most strongly impacts  $\Phi$ , it is the parameter which is measured most accurately;  $\mu$  does not impact  $\Phi$  as strongly and so is not measured as precisely. The phase also depends on the spins that the black holes would have in isolation,  $\mathbf{S}_1$  and  $\mathbf{S}_2$ . We do not fully take this dependence into account; as we discuss in §5 there is room for significant improvement upon our analysis by doing so.

An interesting feature of GW measurements is that they do not actually measure a binary’s masses; rather, they measure *redshifted* mass parameters. This is because any quantity  $m$  with the dimension of mass enters the orbit evolution of the binary as a timescale  $Gm/c^3$ ; this timescale is then redshifted. Hence, we measure  $\mathcal{M}_z \equiv (1+z)\mathcal{M}$  and  $\mu_z \equiv (1+z)\mu$ . As we discuss in detail in §3, this subtlety has no impact on this analysis, although it is crucial for many other studies (see, e.g., Hughes 2002).

The ending of the inspiral is not perfectly well defined in all circumstances, but corresponds roughly to when the members of the binary are separated by a distance  $r \sim 6GM/c^2$ . At this separation, the system’s evolution will certainly cease being slow and adiabatic; the black holes will plunge towards one another and merge into a single object.

## 2.2. Ringdown

The ringdown epoch consists of the last waves the system generates, as the merged remnant of the coalescence relaxes to the quiescent Kerr black hole state. As it settles down, the distortions to this final black hole can be decomposed into spheroidal modes, with spherical-harmonic-like indices  $l$  and  $m$ ; the evolution of these modes can then be treated using perturbation theory (Leaver 1985). Each mode takes the form of a damped sinusoid. Once the indices are fixed, the frequency and damping time of these modes is determined by the final mass and spin of the merged black hole:

$$h_{\text{ring}}(t) \propto \exp(-\pi f_{\text{ring}} t / Q) \cos(2\pi f_{\text{ring}} t + \varphi) . \quad (3)$$

The indices most likely are fixed to  $l = m = 2$ . This is a bar-like mode oriented with the hole’s spin. Since a coalescing system has a shape that nearly mimics this mode’s shape, it should be preferentially excited; also, it is more long-lived than other modes. A good fit for this mode’s frequency  $f_{\text{ring}}$  and quality factor  $Q$  is (Leaver 1985, Echeverria 1989)

$$f_{\text{ring}} = \frac{1}{2\pi(1+z)M_f} [1 - 0.63(1-a)^{3/10}] , \quad (4)$$

$$Q_{\text{ring}} = 2(1 - a)^{-9/20} . \quad (5)$$

The parameter  $(1 + z)M_f$  is the redshifted mass of the final, merged remnant of the binary;  $a = |\mathbf{S}_f|/M_f^2$  is the dimensionless Kerr spin parameter of the remnant, calculated from its spin vector  $\mathbf{S}_f$ .

Measurement of the ringdown waves thus makes it possible to determine the final mass of the merged system. We set the amplitude of this mode by assuming that 1% of the system’s mass is converted into GWs during the ringdown. This is consistent with (or somewhat smaller than) results seen in recent numerical simulations [see, e.g., Baker et al. (2001) and references therein]. For the most part, our results are only weakly dependent on this choice. If the radiated fraction is smaller than 1% by more than a factor of a few, then in some cases (particularly on the lower-mass end of the golden range we discuss below), the final mass will not be determined well enough for measurements to be golden.

The ringdown waves also allow us to determine the magnitude of the merged system’s spin angular momentum,  $|\mathbf{S}_f|$ . We will not take advantage of this feature in this analysis. As we discuss in §5, measurement of  $|\mathbf{S}_f|$  could play an important role in an extension to our basic idea.

### 2.3. Merger

The “merger” epoch consists of all GWs generated between the inspiral and ringdown. Physically, this epoch describes the phase in which the evolution ceases to be slow and adiabatic. At least for large mass ratio, the members of the binary encounter a dynamical instability in their orbit and rapidly plunge together, merging into a highly distorted object. Because of the extreme strong field nature of this epoch, neither a straightforward application of post-Newtonian theory nor perturbation theory is very useful.

As discussed in the introduction, numerical and analytic work to understand the merger epoch and the transition from inspiral to merger is currently very active. It is certainly to be hoped that, by the time *LISA* flies, the GWs from this regime of coalescence will be well understood for at least some important subsets of possible binary black hole coalescences. At present, the regime we call “merger” is not modeled well enough to contribute to this analysis. Indeed, there may not even be a very useful delineation between “inspiral” and “merger” when  $m_1 \simeq m_2$  — the binary may smoothly evolve from two widely separated bodies into a single object without encountering any kind of instability or sharp transition (e.g., Pfeiffer, Cook, & Teukolsky 2002). However — and this is one of the major results of our analysis — for the golden binaries, we will be able to robustly constrain the GWs emitted from this

regime solely from the inspiral and ringdown waves, without needing detailed modeling of the merger.

### 3. Mass Measurement Accuracy

Hughes (2002) has generated detailed Monte-Carlo simulations to assess the precision with which *LISA* will measure BH masses in a cosmological context. Here we summarize the method and results, and describe how the procedure was extended to estimate the precision on mass deficit measurements for golden binary mergers.

#### 3.1. Mass deficit measurement accuracy: Formalism

We estimate the accuracy with which *LISA* can measure binary black hole parameters using a maximum likelihood parameter estimation formalism originally developed in the context of GW measurements by Finn (1992). We begin with a parameterized model for the GW, written schematically  $h(\boldsymbol{\theta})$ , where  $\boldsymbol{\theta}$  denotes a vector whose components  $\theta^a$  represent the masses of the black holes, their spins, the position of the binary on the sky, etc. From this model and from a description of *LISA*'s sensitivity to GWs, we then build the Fisher information matrix  $\Gamma_{ab}$ . Schematically, this matrix is given by

$$\Gamma_{ab} = 4\text{Re} \int_0^\infty df \frac{\partial_a \tilde{h}^*(f) \partial_b \tilde{h}(f)}{S_h(f)}. \quad (6)$$

The function  $S_h(f)$  is the detector's noise spectral density, which we discuss in more detail below;  $\tilde{h}(f)$  is the Fourier transform of  $h(t)$ , and  $\partial_a \equiv \partial/\partial\theta^a$ . The \* superscript denotes complex conjugate. For detailed discussion of how we compute  $\Gamma_{ab}$ , see Hughes (2002); that paper in turn relies heavily upon the discussion in Cutler (1998), Poisson & Will (1995), Cutler & Flanagan (1994), and Finn & Chernoff (1993). Note in particular that we describe the *LISA* response using the formalism developed by Cutler, which synthesizes a pair of “effective detectors” from the data on the three *LISA* arms; see Cutler (1998) for details.

The inverse Fisher matrix gives us the accuracy with which we expect to measure the parameters  $\theta^a$ :

$$\Sigma^{ab} = \langle \delta\theta^a \delta\theta^b \rangle = (\boldsymbol{\Gamma}^{-1})^{ab}. \quad (7)$$

In this equation,  $\delta\theta^a$  is the measurement error in  $\theta^a$ ; the angle brackets denote an ensemble average over all possible realizations of noise produced by the detector. Thus, the diagonal components,  $\Sigma^{aa} = \langle (\delta\theta^a)^2 \rangle$ , represent the expected squared errors in a measurement of  $\theta^a$ ; off-diagonal components describe correlations between parameters.

For our purposes, the most important result is that for golden binaries, we measure the chirp mass  $\mathcal{M}$ , the reduced mass  $\mu$ , and the final mass of the merged system  $M_f$ . From these, we construct the GW mass deficit  $M_{\text{GW}}$ . As discussed in the previous section, we would actually measure *redshifted* mass parameters,  $(1+z)\mathcal{M}$ ,  $(1+z)\mu$ ,  $(1+z)M_f$ , and  $(1+z)M_{\text{GW}}$ . The redshift is irrelevant to us here: since all of our masses are measured at the same  $z$ , the factor  $1+z$  is an uninteresting overall rescaling. We will present all of our error estimates in dimensionless form ( $\delta\mathcal{M}/\mathcal{M}$ ,  $\delta M_{\text{GW}}/M$ , etc.), so that this dependence scales out. This has the important effect that uncertainties in cosmological parameters do not effect our analysis.

Since  $\mathcal{M}$  and  $\mu$  depend upon the masses of the two black holes which constitute the binary, we infer the initial total mass of the system  $M_i$  from  $\mathcal{M}$  and  $\mu$ : using the definition  $\mathcal{M} = \mu^{3/5} M_i^{2/5}$ , we have

$$M_i = \mu^{-3/2} \mathcal{M}^{5/2} . \quad (8)$$

From the difference between  $M_i$  and  $M_f$ , we then infer how much of the system’s mass was radiated in GWs:

$$M_{\text{GW}} \equiv M_i - M_f . \quad (9)$$

Our goal is to assess what errors  $\delta M_{\text{GW}}$  are likely. The mass loss is itself a fairly small quantity — we expect  $M_{\text{GW}}/M \lesssim 10 - 20\%$  at best. Clearly, the ratio  $\delta M_{\text{GW}}/M$  must be smaller than this if the measurement of  $M_{\text{GW}}$  is to have any meaning. We now relate  $\delta M_{\text{GW}}$  to the errors  $\delta\mathcal{M}$ ,  $\delta\mu$ , and  $\delta M_f$  estimated by our Monte-Carlo calculations.

Because the inspiral and ringdown epochs are likely to be analyzed separately, our estimates of  $M_i$  and  $M_f$  should be statistically independent of one another. The errors in these quantities thus combine in quadrature for the error  $\delta M_{\text{GW}}$ :

$$\delta M_{\text{GW}}^2 = \delta M_i^2 + \delta M_f^2 . \quad (10)$$

Since  $M_i \simeq M_f \simeq M$ , it is convenient to divide by the mass of the system to write this as

$$\left( \frac{\delta M_{\text{GW}}}{M} \right)^2 \simeq \left( \frac{\delta M_i}{M_i} \right)^2 + \left( \frac{\delta M_f}{M_f} \right)^2 . \quad (11)$$

This allows us to scale out the uninteresting  $(1+z)$  factor attached to all masses. Also, our Monte-Carlo code’s estimates of error in any mass parameter  $m$  are given in the form  $\delta \ln(m) = \delta m/m$ ; see Hughes (2002) for details.

Using Eq. (8), we find the following relation for the error  $\delta M_i$  in terms of errors in the chirp and reduced masses:

$$\left( \frac{\delta M_i}{M_i} \right)^2 \simeq \left( \frac{\partial M_i}{\partial \mu} \right)^2 \left( \frac{\delta \mu}{M_i} \right)^2 + \left( \frac{\partial M_i}{\partial \mathcal{M}} \right)^2 \left( \frac{\delta \mathcal{M}}{M_i} \right)^2$$

$$\simeq \frac{9}{4} \left( \frac{\delta\mu}{\mu} \right)^2 + \frac{25}{4} \left( \frac{\delta\mathcal{M}}{\mathcal{M}} \right)^2. \quad (12)$$

Our final expression for the error in  $M_{\text{GW}}$ , normalized to the total mass of the binary, is thus

$$\frac{\delta M_{\text{GW}}}{M} \simeq \left[ \frac{9}{4} \left( \frac{\delta\mu}{\mu} \right)^2 + \frac{25}{4} \left( \frac{\delta\mathcal{M}}{\mathcal{M}} \right)^2 + \left( \frac{\delta M_f}{M_f} \right)^2 \right]^{1/2}. \quad (13)$$

We build the likely distributions of this error parameter through Monte-Carlo simulation. We choose masses for the binaries’ members, we choose the binaries’ redshift, and we then randomly distribute such binaries in sky position, source orientation, and final merger time.

Our procedure for doing this analysis is nearly identical to that described in §4 of Hughes (2002), so we will not discuss it in detail here. We do note two important differences between Hughes (2002) and this analysis. First, we include here the effect of mass ratio. Hughes (2002) focused, for simplicity, on equal mass binaries. For a fair assessment of the likely importance of golden binaries, inclusion of mass ratio is necessary. Second, we have updated the description of the *LISA* noise  $S_h(f)$ ; we now use the sensitivity described by Barack and Cutler (2004) [their Eqs. (48)–(54)]. This corrects some errors in Hughes (2002) and is in accord with current plans for the *LISA* mission.

We make one modification to Barack and Cutler’s noise curve: we assume that the detector’s response is only well-understood above some fiducial frequency  $f_{\text{low}}$ , so that we ignore all GWs that radiate at  $f < f_{\text{low}}$ . During the inspiral, a binary’s orbital frequency monotonically increases as its black holes gradually fall towards one another. By ignoring waves with  $f < f_{\text{low}}$ , we are effectively saying that a signal becomes visible to *LISA* when its GW frequency becomes greater than  $f_{\text{low}}$ . An appropriate value for  $f_{\text{low}}$  is a matter of some debate; physically, we expect that  $f_{\text{low}} \simeq 2\pi/T_{\text{DF}}$ , where  $T_{\text{DF}}$  is the maximum time over which the *LISA* spacecraft can maintain “drag-free” orbital motion. Much work on *LISA* science assumes that  $f_{\text{low}} \simeq 10^{-4}$  Hz; the *LISA* science team is currently investigating whether the noise can be characterized down to  $f_{\text{low}} \simeq 3 \times 10^{-5}$  Hz. Lower values of  $f_{\text{low}}$  typically lead to improved accuracy for parameters of the inspiral waveform, since more phase is measured (see Hughes & Holz 2003, Figure 2); this can be particularly important for higher black hole masses, since GW frequencies are inversely proportional to mass.

In the results that we present here, we have set  $f_{\text{low}} = 3 \times 10^{-5}$  Hz, assuming (perhaps optimistically) that the instrument’s noise will be well-characterized to relatively low frequencies. We have also examined golden binaries for the choice  $f_{\text{low}} = 10^{-4}$  Hz. Though we do not discuss these results in detail, the impact of this choice can be simply summarized: the accuracy with which both the chirp mass  $\mathcal{M}$  and the reduced mass  $\mu$  are measured is

degraded. The degradation in  $\mathcal{M}$  is not important —  $\mathcal{M}$  is determined so precisely that it is largely irrelevant in setting the accuracy with which  $M_{\text{GW}}$  is determined. We typically find  $\delta\mathcal{M}/\mathcal{M} \sim 10^{-3} - 10^{-4}$ ; this phenomenal accuracy is because the chirp mass largely determines the number of orbits which are radiated in the detector’s band. A phase coherent measurement is very sensitive to this number, and thus determines  $\mathcal{M}$  very precisely.

By contrast, the degradation in  $\mu$  has a very large effect. In the best cases, we find that  $\mu$  is determined with an accuracy of a fraction of a percent to a few percent; in most cases, it dominates the error budget for  $M_{\text{GW}}$ . When  $f_{\text{low}} = 10^{-4}$  Hz is used instead of  $3 \times 10^{-5}$  Hz, the error in  $\mu$  typically increases by a factor  $\sim 3 - 10$ . This sharply restricts the mass range that can be considered golden. It is likely that this tendency can be offset by taking into account, as in Vecchio (2004), modulations due to spin precessions which break certain degeneracies and allow  $\mu$  to be determined much more accurately.

### 3.2. Mass deficit measurement accuracy: Results

Our Monte-Carlo distributions for  $\delta M_{\text{GW}}$  show that golden binaries exist in a somewhat narrow band of mass, typically from  $M_z \sim \text{several} \times 10^5 M_\odot$  to  $M_z \sim \text{several} \times 10^6 M_\odot$ , where  $M_z = (1 + z)M$ , and  $M$  is the binary’s total mass. Binaries more massive than this do not radiate in band long enough to determine the system’s reduced mass with sufficient accuracy to be golden; less massive binaries do not have a ringdown signal that is loud enough to determine the system’s final mass with sufficient accuracy. The upper and lower bounds on this mass window evolve with redshift, so that the mass window shrinks as we move to higher  $z$ .

Figures 1–5 show representative probability distributions for the measurement error  $\delta M_{\text{GW}}$  as a function of binary masses and redshift. Figures 1 and 2 show results for small redshift,  $z = 0.5$ . Although we do not expect a very interesting event rate at this redshift, this result gives a “best case” illustration of how well these measurements can be performed in principle — events at  $z = 0.5$  are so strong that mass parameters are determined with very high precision. Figure 1 illustrates the “goldenness” of the range  $2 \times 10^5 M_\odot \lesssim M \lesssim 2 \times 10^6 M_\odot$  at this redshift. The most likely error (peak of the distribution)  $\delta M_{\text{GW}}/M$  is about 2 – 3% at the extrema of the range ( $m_1 = m_2 = 10^5 M_\odot$  and  $m_1 = m_2 = 10^6 M_\odot$ ), and goes down to  $\delta M_{\text{GW}}/M \simeq 1\%$  in the best cases.

Although these distributions show a peak representing excellent measurement precision, it must be emphasized that each distribution also has a rather extended, large error tail. These tails are mostly due to a subset of MBH binaries in the Monte Carlo realizations that

have a short inspiral time before coalescence at the time of detection.

As we move to higher and lower masses, the peak of the error distribution shifts outside of the golden range. Figure 2 illustrates the error distributions at  $z = 0.5$  just above and just below the masses shown in Fig. 1. Although there is still a good probability of measuring a golden event at these masses, they are no longer the most likely events. As we move to even higher and lower masses, the probability of a golden event decreases more rapidly.

The rule of thumb we learn from Figs. 1 and 2 is that the most probable mass range for golden binaries are those with a redshifted mass several  $\times 10^5 M_\odot \lesssim M_z \lesssim$  a few  $\times 10^6 M_\odot$ . As Figs. 3 – 5 illustrate, this pattern continues out to  $z \sim 2-4$ . At  $z = 1$ , most of the merger events in this mass range will be golden; see Fig. 3. Beyond this range, the probability that an event is golden begins to decrease, largely due to the weakness of signals at this distance, which makes determining the final mass difficult. Fig. 4 shows the distribution of errors at  $z = 2$ . Many events are still golden at this redshift, though the proportion is decreasing. By the time we reach  $z = 4$  (Fig. 5), the proportion of golden events has fallen quite a bit.

By considering the peaks of the many error distributions that we have computed, we determine a typical range of masses, as a function of redshift, for which binaries are golden (i.e. with a distribution of  $\delta M_{\text{GW}}/M$  peaking at 5% or less). Beyond  $z \sim 4$ , *LISA* cannot determine  $M_{\text{GW}}$  well enough for there to be a reasonable probability of measuring a golden merger; but, a fairly large range of masses are golden at lower redshifts. We find that a simple mass-redshift prescription reproduces our results reasonably well, even though it does not capture all of the information contained in error distributions such as those shown in Figs. 1–5. For a black hole binary to be golden, the largest mass black hole,  $m_1$ , should satisfy the constraint

$$5 < \log \left( \frac{m_1}{M_\odot} \right) < 5 + 1.3 \times \left( \frac{4 - z}{3.5} \right), \quad (14)$$

which results in no binary being classified as golden beyond  $z = 4$ . In addition, the lowest mass black hole,  $m_2$ , should satisfy the constraint

$$0.3 \leq q \equiv m_2/m_1 \leq 1. \quad (15)$$

This constraint on the binary mass ratio is partly the result of our error analysis (binaries with small mass ratios are often not golden). It is also motivated by the expectation that radiative mass losses,  $M_{\text{GW}}/M$ , are small in mergers with fairly unequal masses. While losses can perhaps reach  $\sim 10-20\%$  in a binary with  $q \sim 1$  (depending on the spins and relative orientations of the merging BHs), an expected  $q^2$  scaling for the losses makes it unlikely that  $M_{\text{GW}}$  can be measured in binaries with small mass ratios (see, e.g., Menou & Haiman 2004 and references therein for a discussion of these scalings). We have chosen  $q = 0.3$  as a limit below which losses (likely  $< 1-2\%$ ) become very difficult to measure with *LISA*.

Having demonstrated the possibility of radiative mass loss measurements with *LISA*, it remains to be seen whether enough golden binary mergers satisfying the above constraints will occur for *LISA* to actually carry out any such measurement. Using specific population models, we argue in the next section that the event rate of golden binary mergers is rather low, but nonetheless high enough that  $M_{\text{GW}}$  measurements are plausible for a nominal 3-year *LISA* mission lifetime.

#### 4. Population Models and Event Rates

At present, too little is known about the characteristics of the population of MBHs at cosmological distances to make robust merger rate predictions for *LISA*. Here, our goal is to show that one may reasonably expect *LISA* to make some radiative mass loss measurements from golden binaries. To do so, we rely on pre-existing population models, which were described at length in Menou et al. (2001) and Menou (2003). Though simple, these models capture the essential galactic merger process which is at the origin of MBH coalescences. Let us summarize here their main characteristics.

The basic ingredient of these models is a “merger tree” describing the cosmic evolution of dark matter halos in a concordance  $\Lambda$ -CDM cosmology (Press & Schechter 1974; Lacey & Cole 1993, 1994). Unless otherwise specified, all model parameters adopted here are identical to those in Menou et al. (2001). By identifying dark matter halos with individual galaxies and by populating these galaxies with central MBHs, it is possible to follow the cosmic evolution of galactic mergers and trace the occurrence of MBH coalescences through cosmic times.

While this simple description of galactic and MBH mergers has received some basic observational support (see, e.g., Komossa et al. 2003), it also hides a number of complications and related uncertainties. Even though dynamical studies indicate that nearly all nearby massive galaxies harbor central MBHs (Magorrian et al. 1998), it is unclear how frequently these MBHs are present in galaxies at higher redshifts (Menou et al. 2001; Volonteri, Haardt & Madau 2003). In addition, the timescale on which two MBHs coalesce, within a merged galactic remnant, is not well known. Dynamical friction is the initial mechanism bringing the two MBHs together, but the timescale on which it operates becomes increasingly long for small mass ratios (Yu 2002). The second mechanism bringing the two MBHs together, which involves three-body encounters with stars on very low angular momentum orbits (in the “loss cone”), may be rather inefficient (see, e.g., Begelman, Blandford & Rees 1980; Milosavljevic & Merritt 2003). On the other hand, interaction between the two MBHs and a gaseous component may help accelerate their coalescence substantially (e.g. Gould & Rix

2000; Escala et al. 2004). To assess the likelihood of *LISA* performing accurate mass loss measurements over its mission lifetime, we will focus on an optimistic scenario in which it is assumed that MBHs coalesce efficiently following the merger of their host galaxies. We will then comment on the consequences of relaxing this assumption for our results.

We must specify the mass properties of the cosmological population of MBHs in our models. In recent years, spectacular progress has been made in characterizing the masses of MBHs at the centers of nearby galaxies. A tight correlation between BH mass and velocity dispersion of the galactic spheroidal component has been established via detailed dynamical studies (Gebhardt et al. 2000; Ferrarese & Merritt 2000; Tremaine et al. 2002). A relation between BH mass and galactic mass has subsequently been proposed (Ferrarese 2002). Evidence that this link between central MBHs and their host galaxies is already in place at redshifts  $z \sim 3$  has also been presented (Shields et al. 2003), although more recent work suggests that this link may evolve rather significantly (Treu, Malkan, & Blandford 2004).

In view of these developments, we assume that the following relation between the galactic mass and the BH mass,  $M_{\text{bh}}$ , is satisfied at all times in our population models (Ferrarese 2002; Wyithe & Loeb 2004):

$$M_{\text{bh}} = 10^9 M_{\odot} \left( \frac{M_{\text{halo}}}{1.5 \times 10^{12} M_{\odot}} \right)^{5/3} \left( \frac{1+z}{7} \right)^{5/2}, \quad (16)$$

where  $M_{\text{halo}}$  is the mass of the dark matter halo associated with each galaxy. This relation may result from radiative or mechanical feedback by the quasar during active periods of BH mass accretion (e.g. Silk & Rees 1998; Murray, Quataert & Thompson 2004). We do not explicitly model BH accretion in our models, but it is done implicitly by enforcing the above relation for all MBHs, at all epochs.

Equipped with this population model, it is now possible to calculate the merger rate of MBH binaries, including the subset of binaries satisfying the “golden” conditions given in Eqs. (14) and (15). We consider two separate models, starting at  $z = 5$ . In one model, we assume that MBHs are abundant in the sense that all potential host galaxies at  $z = 5$  do harbor a MBH. In a second model, we assume that MBHs are  $\sim 30$  times rarer, by confining them to the 3% most massive galaxies described by the merger tree at  $z = 5$ . This was found to be about the lowest occupation fraction at that redshift which remains consistent with the observational requirement of ubiquitous MBHs in massive galaxies at  $z = 0$  by Menou et al. (2001). Apart from assigning a mass to each MBH (Eq. [16]), our models are thus identical to two of the three models discussed in detail in Menou et al. (2001).

Figure 6 shows the event rates for golden binary mergers predicted by these two models

(after averaging over ten independent realizations of the merger tree). The dashed line corresponds to the model with abundant MBHs and the dotted line to the model with rare MBHs. For comparison, we also show the total event rate in the model with rare MBHs as a solid line (same as in Fig. 2b of Menou et al. 2001). As expected from our “goldenness” definition, the rate of golden binary mergers falls precipitously at  $z \sim 3.5-4$ . In both models, it peaks around  $z \sim 2-3$ , where it reaches  $\sim 1\%$  of the total merger rate in the model with abundant MBHs (not shown) and  $\sim 10\%$  of the total merger rate in the model with rare MBHs (compare solid and dotted lines).

In the model with abundant MBHs, the total number of golden events, integrated over all redshifts, adds up to  $N_{\text{gold}} \sim 5$  for a 3-year *LISA* mission lifetime. It reduces to  $N_{\text{gold}} \sim 1$  in the model with rare MBHs. These numbers are encouraging because they suggest that *LISA* can reasonably be expected to perform one or several accurate radiative mass loss measurements. Of course, one should also keep in mind that our models are partly optimistic in assuming efficient MBH coalescences after galactic mergers. The lower efficiency of dynamical friction at low mass ratios should not affect much our predictions for golden binary mergers because we have restricted golden binaries to have mass ratios  $q \geq 0.3$  (Eq. [15]). But, if MBH coalescences are much less efficient than assumed here, because of the difficulty in replenishing “loss cones” and of the absence of an accelerating gaseous component, merger rates for binaries of all types could be well below our predictions. This could make the occurrence of golden events rather unlikely. In that case, it may also be the case that the total event rate for *LISA* would turn out to be a disappointingly low number. On the other hand, it should be borne in mind that we have been somewhat conservative in our estimates of how precisely masses can be measured. The range of binary mass that can be considered golden is probably somewhat broader than we have assumed, which may offset somewhat any loss in the rate of golden events.

## 5. Discussion and Conclusion

Within a certain mass range, *LISA* will be able to measure the GWs that come from all epochs of the binary black hole coalescence process. By precisely measuring the initial and final masses of the system, *LISA* will determine how much of the system’s mass is radiated away. Such a measurement will constitute an extremely interesting and robust probe of strong-field general relativity.

As we have emphasized, a particularly interesting feature of these “golden” binaries is that the mass deficit can be determined without a detailed model of the highly dynamical, strong field plunge and merger epoch. Although it is almost certain that our theoretical

understanding of this epoch will be much improved by the time *LISA* flies, we should not be surprised if substantial uncertainties remain in the *LISA* era. A simple and robust measure of strong-field physics such as  $M_{\text{GW}}$  can play a particularly important role in developing a phenomenology of binary black hole merger physics. Such an observable may be useful as a kind of global calibration on the process, even if the waveform models for the plunge/merger regime can not be computed with good accuracy.

We also emphasize again that our estimates for the accuracy with which  $M_{\text{GW}}$  will be measured are, in all likelihood, somewhat pessimistic. Especially for the larger masses, much of our error  $\delta M_{\text{GW}}$  is due to a (relatively) poorly determined value of the binary’s reduced mass  $\mu$ . Parameter measurement analyses of post-Newtonian waveforms have shown such large uncertainties are typically due to correlations between  $\mu$  and so-called “spin-orbit” and “spin-spin” parameters — parameters which depend upon couplings between the binary’s orbital angular momentum and black hole spin vectors (Cutler & Flanagan 1993, Poisson & Will 1995). Vecchio (2004) has shown that these correlations can be broken by carefully taking into account spin-induced modulations in the orbital motion of the binary and their influence upon the gravitational waveform. In some cases, the error  $\delta\mu$  can be reduced by an order of magnitude or better. The range of golden binaries thus likely extends to somewhat larger masses than we have estimated, improving the likelihood that *LISA* will measure these events. This effect may also allow binaries to be measured with “golden” precision even if our description of *LISA*’s low-frequency noise turns out to be too optimistic.

Taking into account spin-induced precessions not only reduces the error with which  $\mu$  is measured; it also makes possible a determination of the binary’s individual black hole spins,  $\mathbf{S}_1$  and  $\mathbf{S}_2$ . As we mentioned in §2, ringdown waves allow us to determine the merged remnant’s spin magnitude  $|\mathbf{S}_f|$  as well as its mass; in fact, spin and mass are measured with essentially the same relative precision (Finn 1992). This suggests another extremely interesting measurement that might be possible with these binaries: demonstrating that the initial and final configurations of the system satisfy the *area theorem* (Hawking 1971). Although the mass of the system must decrease because of radiative losses,

$$M_i = M_1 + M_2 > M_f , \tag{17}$$

the area of all event horizons in the system must *increase* during the coalescence:

$$A_i = A_1 + A_2 < A_f . \tag{18}$$

The area of a black hole’s event horizon is determined totally by its mass and angular momentum:

$$A = 8\pi M^2 \left( 1 + \sqrt{1 - a^2} \right) . \tag{19}$$

(Here,  $a = |\mathbf{S}|/M^2$  is the dimensionless Kerr parameter.) This measurement would demonstrate observationally a fundamental law of black hole physics.

SAH thanks Sterl Phinney, Curt Cutler, and Alberto Vecchio for helpful discussions. He also thanks Kip Thorne for a helpful conversation which led us to consider the possibility of golden binaries testing the area theorem. KM thanks Zoltan Haiman for the use of output data from his merger tree code. This work was supported at MIT by NASA Grant NAG5-12906 and by NSF Grant PHY-0244424.

## REFERENCES

- Baker, J., Brüggmann, B., Campanelli, M., Lousto, C., and Takahashi, R. 2001, *Phys. Rev. D*, 49, 6274
- Barack, L. & Cutler, C. 2004, *Phys. Rev. D*, 69, 082005
- Baumgarte, T. W. & Shapiro, S. L. 2003, *Phys. Rep.*, 376, 41
- Begelman, M. C., Blandford, R. D., & Rees, M. J. 1980, *Nature*, 287, 307
- Blanchet, L. 2002, *Living Rev. Relativity*, 5, 3
- Brüggmann, B., Tichy, W. & Jansen, N. 2004, *Phys. Rev. Lett.*, 92, 211101
- Cutler, C. 1998, *Phys. Rev. D*, 57, 7089
- Cutler, C. & Flanagan, E. E. 1994, *Phys. Rev. D*, 49, 2658
- Davis, M., Ruffini, R., Press, W. H., and Price, R. P. 1971, *Phys. Rev. Lett.*, 27, 1466
- Damour, T. 2001, *Phys. Rev. D*, 64, 124013
- Escala, A., Larson, R. B., Coppi, P. S. & Mardones, D. 2004, *ApJ*, 607, 765
- Ferrarese, L. 2002, *ApJ*, 578, 90
- Ferrarese, L. & Merritt, D. 2000, *ApJ*, 539, L9
- Finn, L. S. 1992, *Phys. Rev. D*, 46, 5236
- Finn, L. S. & Chernoff, D. 1993, *Phys. Rev. D*, 47, 2198
- Gebhardt, K. et al. 2000, *ApJ*, 539, L13

- Gould, A. & Rix, H.-W. 2000, *ApJ*, 532, L29
- Haehnelt, M. G. 1994, *MNRAS*, 269, 199
- Hawking, S. W. 1971, *Phys. Rev. D*, 26, 1344
- Hughes, S. A. 2002, *MNRAS*, 331, 805
- Hughes, S. A. & Holz, D. E. 2003, *Class. Quant. Grav.*, 20, S65
- Islam, R. R., Taylor, J. E. & Silk, J. 2004, *MNRAS*, 354, 629
- Komossa, S. et al. 2003, *ApJ*, 582, L15
- Lacey, C. & Cole, S. 1993, *MNRAS*, 262, 627
- Lacey, C. & Cole, S. 1994, *MNRAS*, 271, 676
- Leaver, E. W. 1985, *Proc. R. Soc. Lond. A*, 402, 285
- Magorrian, J. et al. 1998, *AJ*, 115, 2285
- Menou, K. 2003, *Class. Quant. Grav.*, 20, S37
- Menou, K. & Haiman, Z. 2004, *ApJ*, 615, 130
- Menou, K., Haiman, Z. & Narayanan, V. K. 2001, *ApJ*, 558, 535
- Milosavljevic, M. & Merritt, D. 2003, *ApJ*, 596, 860
- Murray, N., Quataert, E. & Thompson, T. A. 2004, *ApJ*, submitted (astro-ph/0406070)
- Nakamura, T., Oohara, K., & Kojima, Y. 1987, *Prog. Theor. Phys. Suppl.*, 90, 1
- Pfeiffer, H. P. , Cook, G. B., & Teukolsky, S. A. 2002, *Phys. Rev. D*, 66, 024047
- Poisson, E. & Will, C. M. 1995, *Phys. Rev. D*, 52, 848
- Press, W. H. & Schechter, P. L. 1974, *ApJ*, 181, 425
- Sesana, A., Haardt, F., Madau, P. & Volonteri, M. 2004a, *ApJ*, 611, 623
- Sesana, A., Haardt, F., Madau, P. & Volonteri, M. 2004b, *ApJ*, submitted (astro-ph/0409255)
- Silk, J. & Rees, M. J. 1998, *A&A*, 331, L1

Treu, T., Malkan, M. A., & Blandford, R. D. 2004, *ApJL*, 615, L97.

Shields, G. et al. 2003, *ApJ*, 583, 124

Vecchio, A. 2004, *Phys. Rev. D*, 70, 042001

Volonteri, M., Haardt, F. & Madau, P. 2003, *ApJ*, 582, 559

Wyithe, J. S. B. & Loeb, A. 2003, *ApJ*, 590, 691

Wyithe, J.S.B. & Loeb, A. 2004, *Nature*, 427, 815

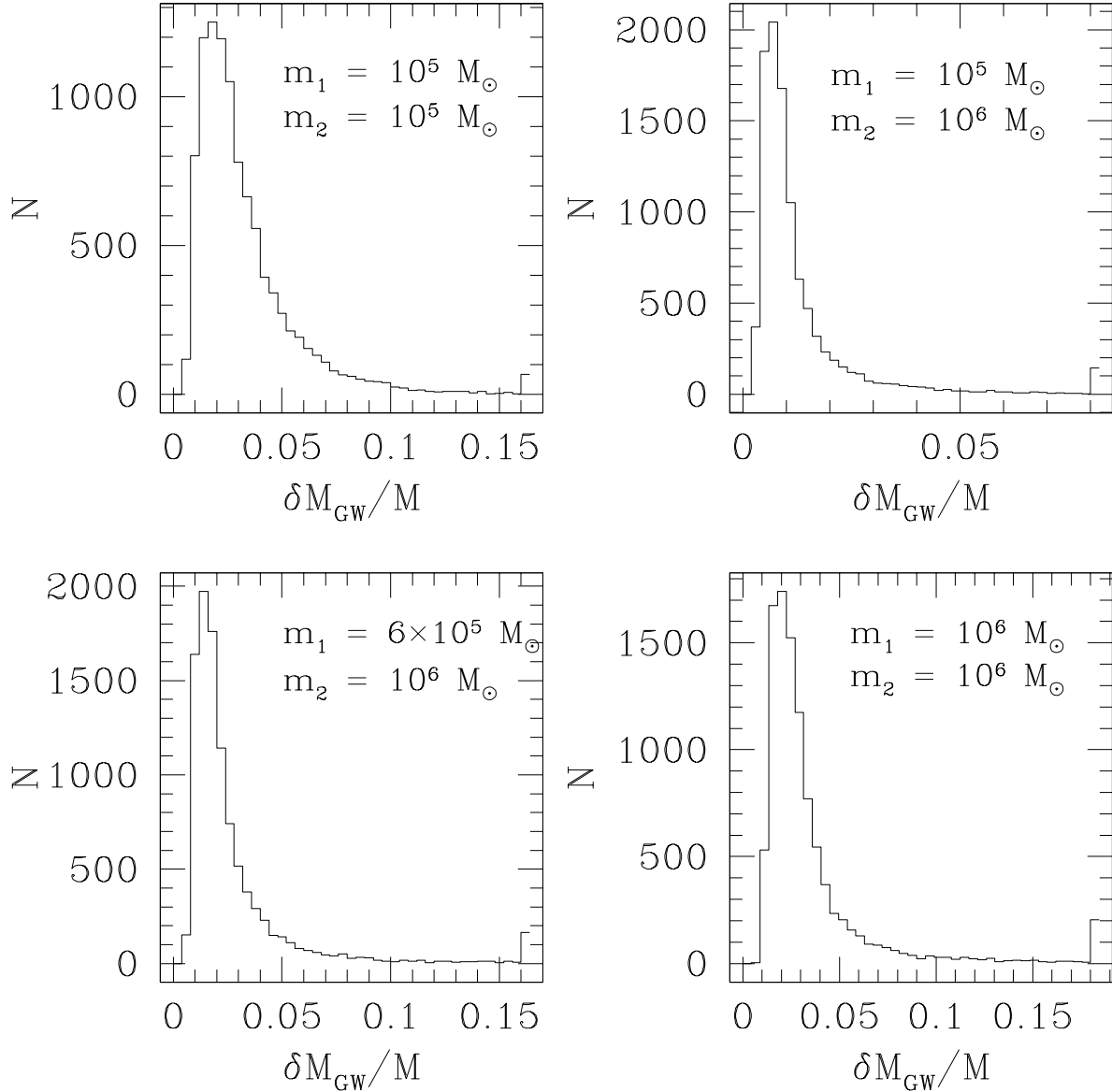


Fig. 1.— Distributions of measurement uncertainty,  $\delta M_{\text{GW}}/M$  (where  $M$  is total binary mass), at  $z = 0.5$ . Each panel represents different choices for the binary masses. As discussed in the text, we randomly populate the sky with 10,000 of these binaries, randomly distributing their orientation vectors and the time at which they coalesce. At this redshift, binaries with these masses are solidly golden: the measurement error distributions peak at relative error of 1% – 3%. We should have little difficulty measuring the mass change due to radiative losses if nature provides us with binaries at these masses and this redshift.

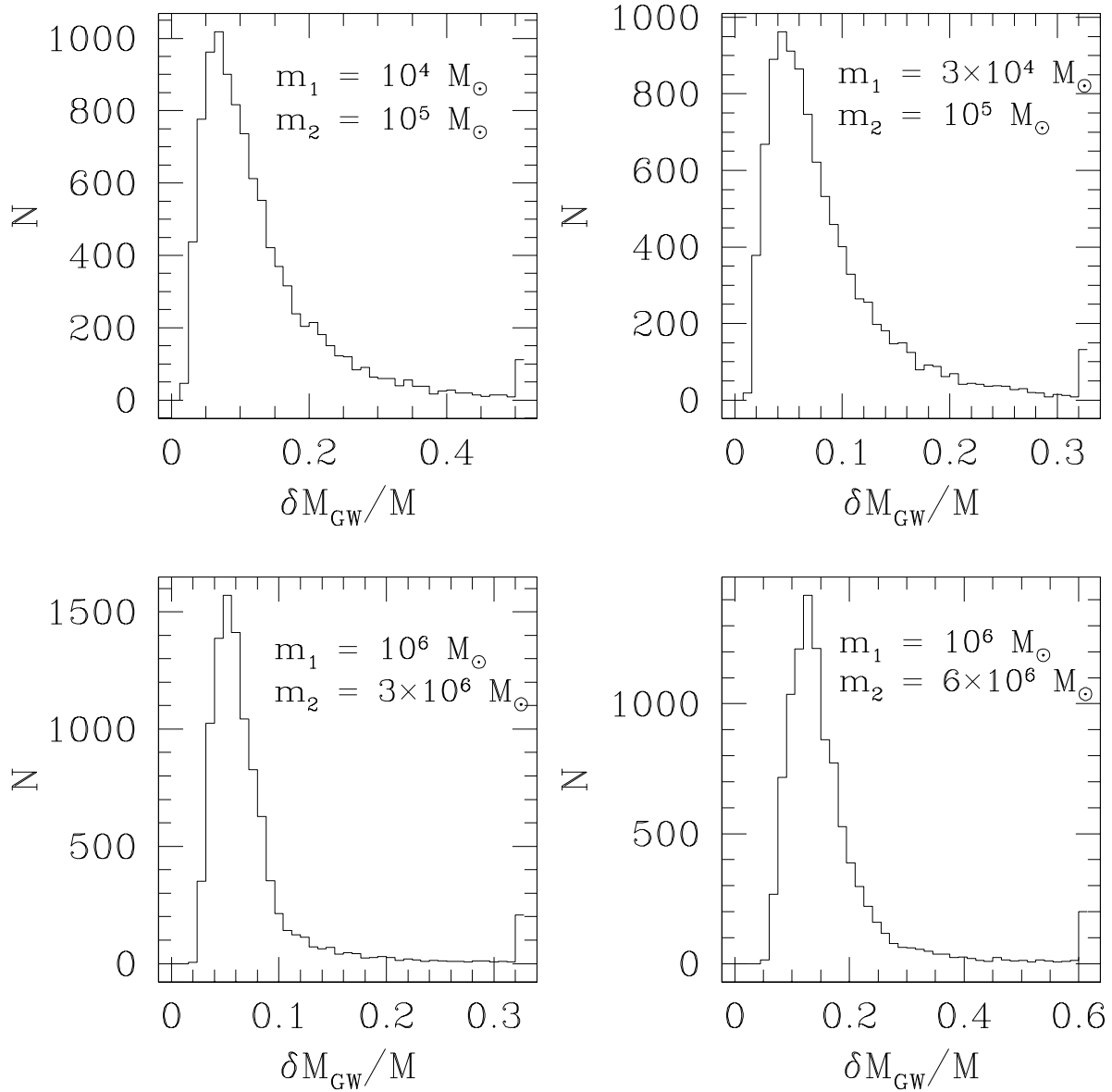


Fig. 2.— Distributions of measurement uncertainty at  $z = 0.5$ . We show here the distribution of measurement uncertainty for binaries just outside the range shown in Fig. 1. As we make the total mass smaller, the final mass becomes more poorly determined due to the weakness of the ringdown signal. As we make the total mass larger, the reduced mass becomes more poorly determined as less time is spent in *LISA*’s band. These distributions peak at a relative error of 5% – 8%; in each case, there is substantial probability for  $\delta M_{\text{GW}}/M \lesssim 3\%$ , though it is not the most likely outcome. There is thus a reasonable likelihood of golden events in these cases, though with much less certainty than in the mass range shown in Fig. 1. As we decrease and increase the masses further, we find that the likelihood of golden events dwindles very rapidly.

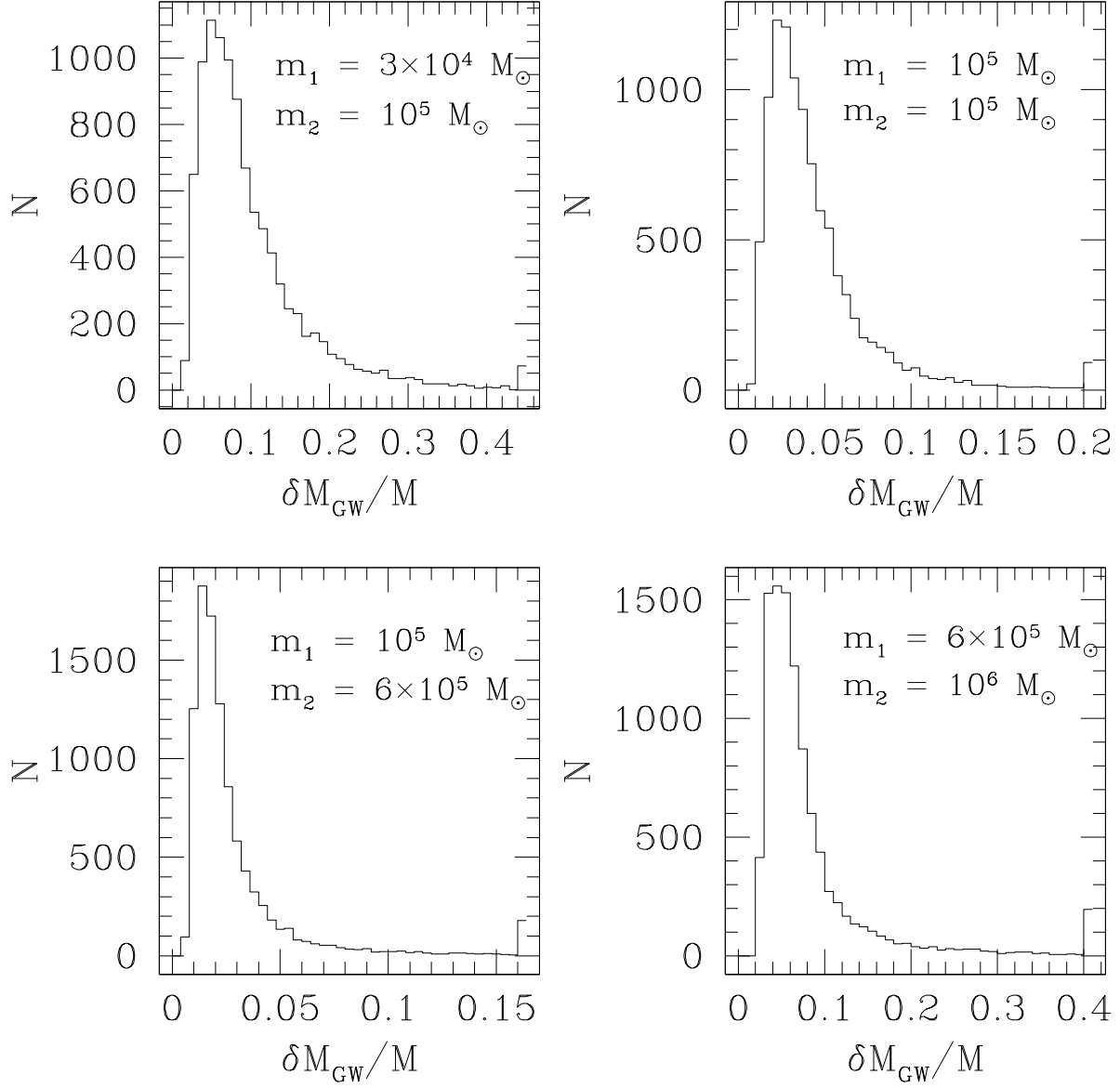


Fig. 3.— Distributions of measurement uncertainty at  $z = 1$ . The mass range containing golden binaries gets smaller, as all signals become weaker at this larger distance, and systematically shifts to somewhat smaller total mass. This shift is in accord with the fact that GW measurements are sensitive to redshifted mass,  $m_z = (1 + z)m$ , for any mass parameter  $m$ . Many events in the mass range shown here are likely to be golden. The likelihood of golden events rapidly falls away as we move outside of this mass range.

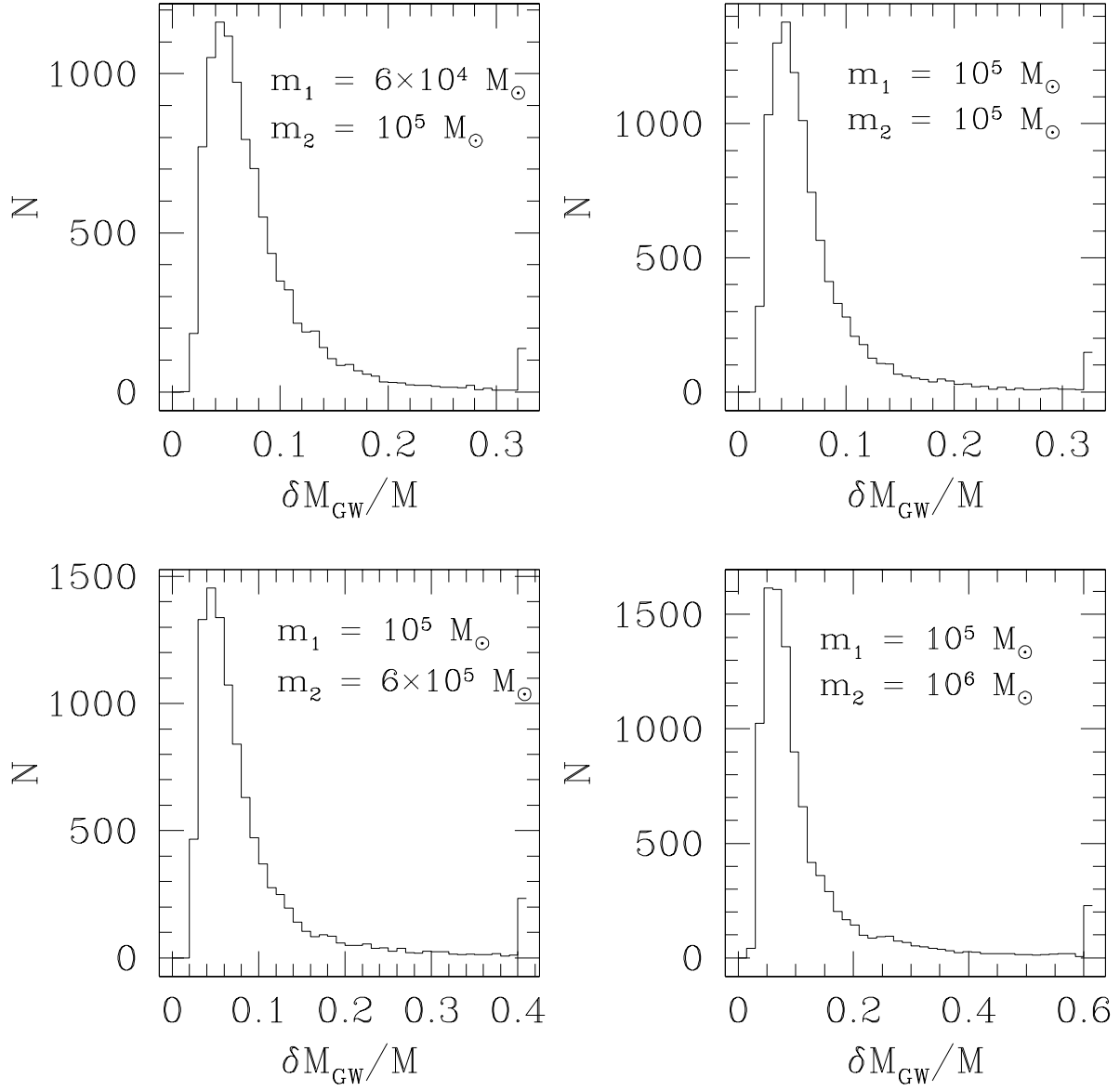


Fig. 4.— Distributions of measurement uncertainty at  $z = 2$ . We continue to see the mass range containing golden binaries getting smaller. Events with total mass  $M \sim \text{several} \times 10^5 M_\odot$  are most likely to be golden at this redshift.

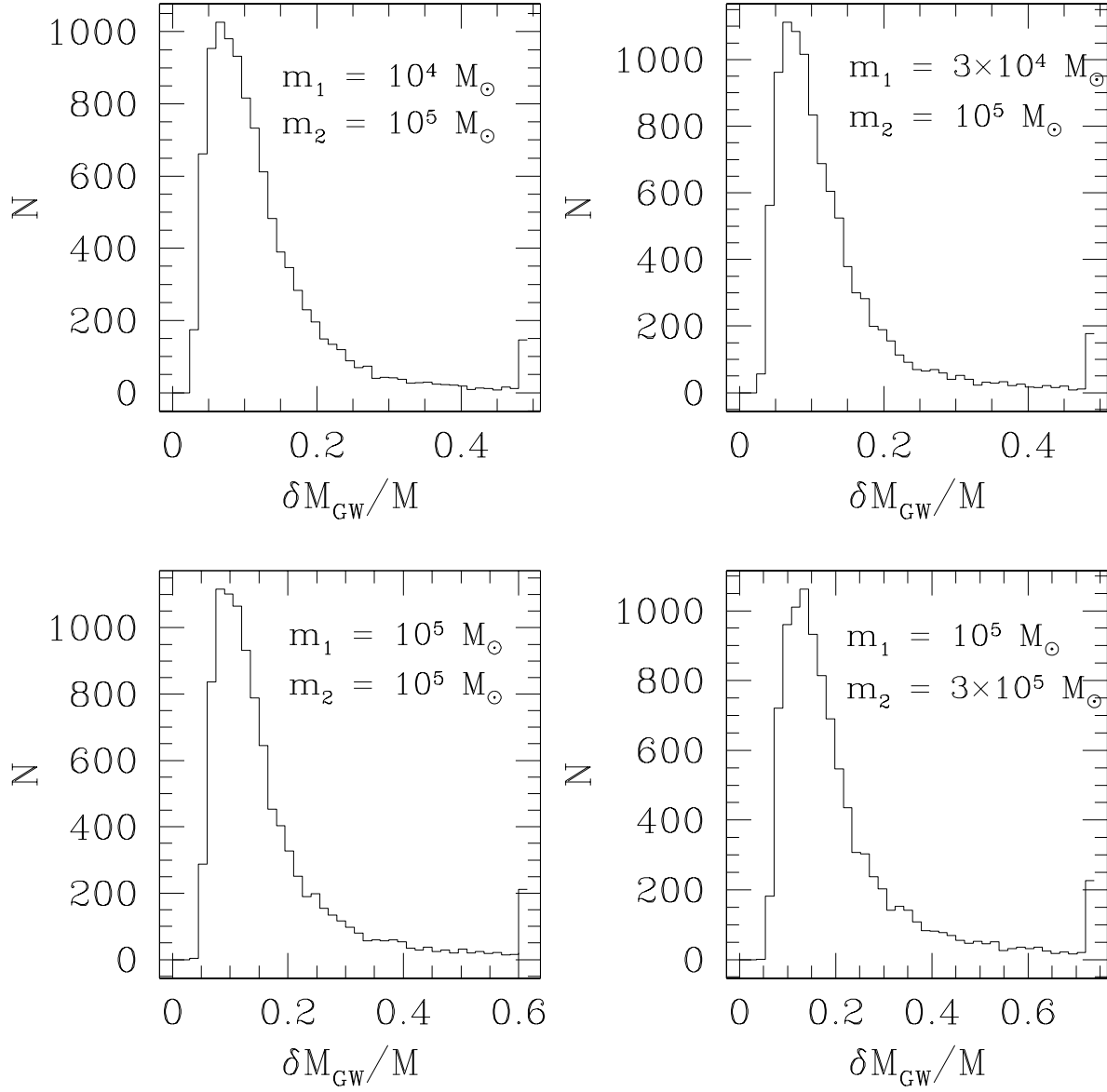


Fig. 5.— Distributions of measurement uncertainty at  $z = 4$ . As we go to these relatively large redshifts, the precision of parameter determination degrades enough that golden events become far less likely — we typically have  $\delta M_{\text{GW}}/M \lesssim 10\%$ , not quite good enough to measure with confidence the radiative mass deficit. Only relatively rare events at this redshift and in this mass regime are expected to be golden.

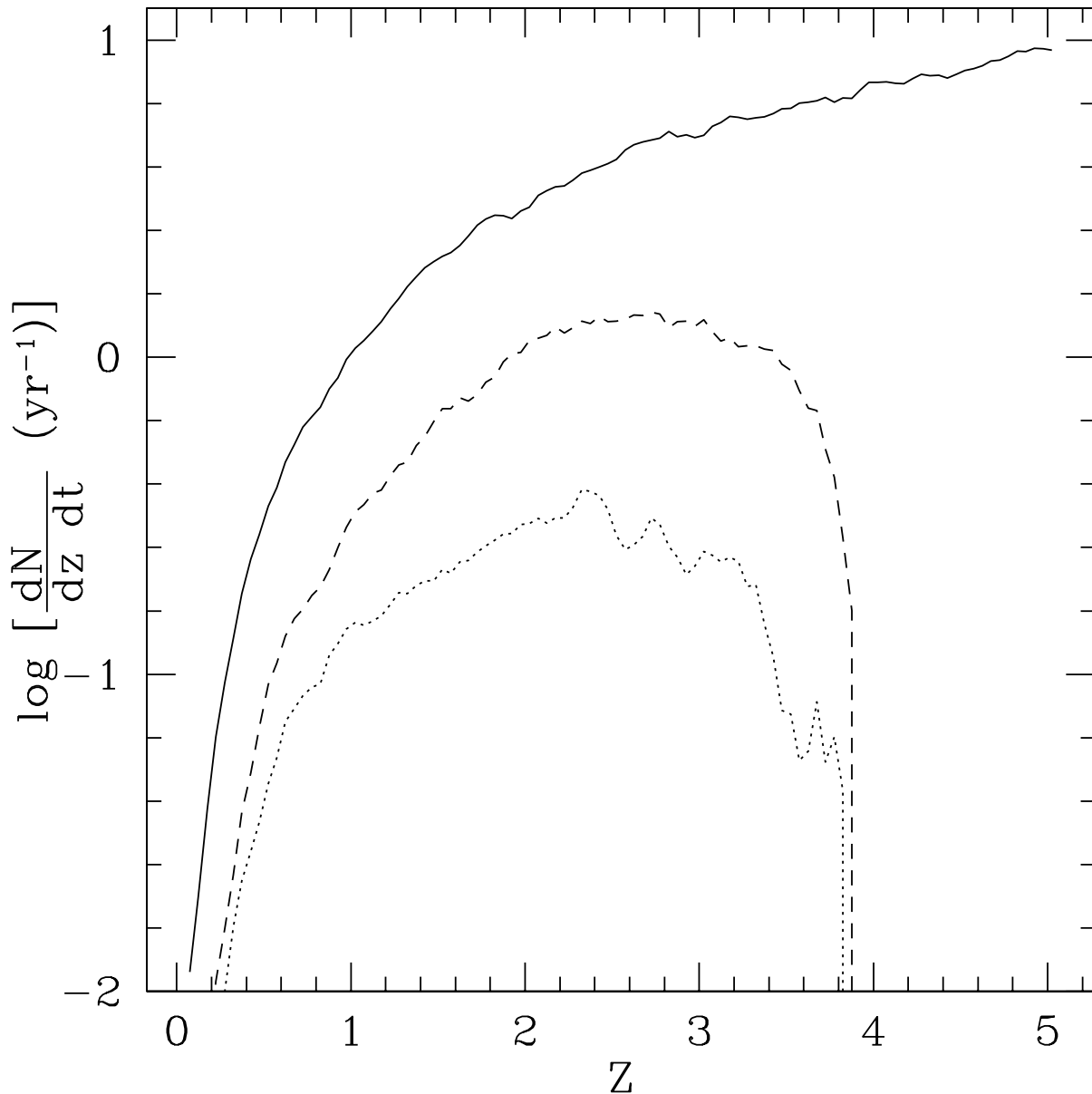


Fig. 6.— Golden binary merger rates for *LISA*, per year and per unit redshift, as a function of redshift,  $z$ . The dashed and dotted lines correspond to models with abundant and rare populations of MBHs, respectively (see text for details). For comparison, the total rate of MBH binary mergers in the model with rare MBHs is also shown as a solid line. All the rates were smoothed over  $\delta z = 0.2$  for better rendering. Integration of these rates over  $z$  and a 3-year *LISA* mission lifetime yields a total of  $N_{\text{gold}} \sim 5$  golden events for the scenario with abundant MBHs and  $N_{\text{gold}} \sim 1$  for the scenario with rare MBHs.